

Chitta R. Patra · Ayelet Odani · Vilas G. Pol ·
Doron Aurbach · Aharon Gedanken

Microwave-assisted synthesis of tin sulfide nanoflakes and their electrochemical performance as Li-inserting materials

Received: 21 October 2005 / Revised: 31 October 2005 / Accepted: 21 November 2005 / Published online: 25 May 2006
© Springer-Verlag 2006

Abstract A novel and quick method has been developed for the preparation of tin sulfide (SnS and SnS₂) nanoflakes in high yield (≈93%) by a microwave irradiation technique for 10–40 min. The sulfides were synthesized in a simple domestic microwave oven (DMO) using stannic chloride and stanous chloride as the precursors of tin and thiourea as the precursor of sulfur in ethylene glycol under argon atmosphere. Elemental sulfur and sodium thiosulfate were also tried as precursors of sulfur. The structures, morphologies, compositions, and physical properties of the products were characterized by powder X-ray diffraction (XRD), differential scanning calorimetry, energy dispersive X-ray analysis, transmission electron microscopy, selected area electron diffraction, Raman spectroscopy, and standard electrochemical techniques. The XRD patterns indicate that the as-synthesized product, obtained after microwave irradiation, is crystalline orthorhombic in the case of the SnS phase and amorphous in the case of SnS₂. Heat treatment of this SnS₂ produced a crystalline hexagonal phase. A possible mechanism for the formation of the tin sulfide nanoflakes is proposed herein. The electrochemical performance of these materials as Li-insertion materials was investigated in a number of electrolyte solutions and was found to be highly sensitive to the solution composition. A stable reversible capacity higher than 600 mAh/g could be obtained with SnS electrodes.

Keywords Tin sulfide nanoflakes · Synthesis · Electrochemistry

Introduction

Metal sulfide semiconductors of nanometer-size dimension are currently recognized as advanced inorganic materials with nonconventional applications due to the quantum size effect exhibited by them [1–4]. Recently, low-dimensional nanostructures, such as nanowires, nanotubes, nanowhiskers, and nanoflakes of semiconductor materials, especially tin sulfides, have attracted much attention due to their possible applications in nanoscale electronic and optoelectronic devices [1, 5, 6]. It has been found that their properties depend on their size and shape, and thus, one of the challenges in nanocrystal synthesis is to control not only the crystal size, but also the particles' shape and morphology [7, 8].

Among metal chalcogenides, tin sulfides (SnS and SnS₂), as IV–VI intermetallic compounds, possess many semiconducting properties. For example, flaky SnS with an orthorhombic structure is a narrow band gap semiconductor with an optical band gap of 1.3 eV, which may be an interesting material for photoelectric energy conversion devices [9, 10]. The high conversion efficiency obtainable from SnS in photovoltaic devices, according to Prince-Loferski diagrams [10–12], and its acceptability in terms of cost, availability, toxicity, and stability, makes this material especially important and interesting.

SnS₂ is also an interesting material that belongs to the class of isomorphous materials that exhibit a strong anisotropy of optical properties [13]. SnS₂ may appear as a layered semiconductor with a band gap of about 2.35 eV [14] and therefore may be useful as a solar cell material [10, 15]. Indeed, SnS₂ is already used in holographic recording systems and electrical switching [16], in photoconducance [17], in solar cells, and in optoelectronic devices [17, 18]. Hence, the unique properties and numerous applications of tin sulfides have stimulated us to develop simple synthetic routes for these materials, in which their morphology (very important for many applications) will be controlled.

Because of the growing importance of SnS and SnS₂ from an academic as well as an industrial point of view,

C. R. Patra · V. G. Pol · A. Gedanken
Department of Chemistry and Kanbar
Laboratory for Nanomaterials at Bar-Ilan University,
Center for Advanced Materials and Nanotechnology,
Bar-Ilan University,
Ramat-Gan 52900, Israel
e-mail: gedanken@mail.biu.ac.il

A. Odani · D. Aurbach (✉)
Department of Chemistry, Bar-Ilan University,
Ramat-Gan 52900, Israel
e-mail: aurbach@mail.biu.ac.il

several authors have reported the synthesis of these materials via different methods. However, the reported conventional methods for the synthesis of these nanomaterials face many kinds of problems: These reported methods take a long time; require high temperature, high pressure, expensive precursors, or template; or needs a special complexing agent. For instance, the production of layered SnS₂ by the interaction of metal carbonyls and H₂S using a microwave plasma technique was reported by Szabó and Vollath [19]. However, metal carbonyls and H₂S are hazardous and poisonous. These problems are the limiting factors in the development of an efficient synthesis of tin sulfides.

In recent years, the use of microwave radiation has been introduced as an efficient tool for the synthesis of materials [20, 21]. Microwave-assisted products may be obtained at high purity, structural uniformity, and high yield. Furthermore, this method does not need a high temperature for the bulk solution (local high temperatures are obtained), high pressure, any catalyst, template, surfactant, vacuum condition, or preprocessing. In addition, this method can be simpler, faster, cleaner, and economically cheaper than other synthetic methods that require stimulating conditions such as heating and pressurizing.

The aim of our present work is to establish an efficient, short, and very simple solvothermal method that avoids the above-mentioned drawbacks for the synthesis of tin sulfides and apply these microwave-synthesized materials (SnS and SnS₂) as Li-insertion materials that can be used as anodes for rechargeable Li batteries. In fact, in parallel to the performance of the work described herein, Chen et al. reported also on the synthesis of SnS and SnS₂ using microwave radiation [22]. However, their study is quite different than the present one, as discussed later in this paper. We should mention previous publications on the electrochemical characterization of SnS₂ materials [23, 24]. There is also a report on the use of SnS as an electrode material in aqueous electric double layer (EDL) capacitors [25]. However, there are no reports on the electrochemical characterization of SnS as an electrode material for rechargeable Li batteries.

Experiments

Sulfur (Aldrich, -100 mesh), sodium thiosulfate (Na₂S₂O₃·5H₂O, Alfa Aesar, 99.5%), thiourea (Merck, 99.5%), tin (IV) chloride (Aldrich, 99% purity), tin(II) chloride (Aldrich, 98% purity), and ethylene glycol (EG) (J.T. Backer Co.) were used as received.

In a typical synthesis of SnS₂, 0.260 g (1 mmol) of tin (IV) chloride and 2 mmol of sulfur source (in a slight excess) were mixed with 40 g of ethylene glycol (an excellent susceptor of microwave radiation, which acts as both solvent and reducing agent) in a 100-ml round-bottomed flask. For SnS synthesis, a typical reaction mixture included 1 mmol of tin(II) chloride and 1 mmol of

thiourea. At room temperature, there was no observable reaction between the above tin and the sulfur sources. The reaction mixtures were purged for half an hour with argon gas, after which the reaction mixtures were irradiated for a certain period of time at approximately 30% of the instrument's power in order to control the reaction and reduce the risk of superheating. These reactions usually produced 140 and 170 mg of as-synthesized SnS and SnS₂, corresponding to 92.8 and 93% yields of SnS and SnS₂, respectively. The entire apparatus, including a modified domestic microwave oven (900 W, with 2.45 GHz), has been described elsewhere [26]. A series of experiments was also carried out separately with different sulfur sources, e.g., elemental sulfur, and sodium thiosulfate instead of thiourea and tin(IV) chloride under similar microwave reaction conditions. No SnS and SnS₂ were formed in these cases. After the reaction, the resulting products were collected, centrifuged, washed with ethanol and distilled water, and then dried overnight under vacuum at room temperature. In order to obtain crystalline SnS₂, the relevant reaction product was annealed under argon for 1 h at 425°C.

Concluding the description of the synthetic part, it should be noted that although the use of microwave ovens in chemical synthesis is relatively elegant and easy compared to synthetic routes that require prolonged heating, this method should be used judiciously.

For instance, *thermal runaway may pose a serious risk*, and hence, the power used has to be adjusted properly (according to the energetics of the expected reactions). Furthermore, when using thiourea as a precursor, its toxicity has to be taken into account.

Electrodes were prepared from a mixture of 85% active material (SnS or SnS₂), 10% carbon black, and 5% polyvinylidene difluoride (PVDF) binder (Solvey, Inc.) by milling for 5 min under air. A slurry was prepared by adding *N*-methyl-2-pyrrolidone (NMP) to the mixture and spreading on copper foils (polished and cleaned in an ultrasonic bath with ethanol and acetone for 15 min followed by drying at 100°C). Finally, the composite thin electrodes were obtained by drying the copper foils containing the uniformly spread slurry at 100°C in an oven for 1 h. Disc-shaped working electrodes, with a diameter of 14 mm, were fabricated. These electrodes were assembled in 2032 coin-type cells (standard products from NRC, Canada) with lithium metal as a counter electrode, separated by a porous polypropylene film. The cycling behavior of tin sulfide and tin disulfide was studied in different electrolyte solutions: 1 M LiPF₆ in ethylene and dimethyl carbonates (EC-DMC), 1 M lithium-bioxalato-borate (LiBOB) in EC-DMC, 1 M LiClO₄ in propylene carbonate (PC), 1 M LiClO₄ in EC:PC 2:3, 1 M LiClO₄ in EC:PC 1:1, and 1 M LiClO₄ in EC:DMC 1:1. LiClO₄ was chosen for these tests because it is one of the least reactive Li salts towards negative electrodes, and it usually does not bring contaminants to the solutions. Li battery grade solvents and solutions were obtained from Merck KGaA

(Germany) and could be used as received. LiBOB was obtained from Cemmetal, Inc. (Germany) and also could be used as received.

The structure and phase purity of the materials were determined by X-ray diffraction (XRD) analysis using a Bruker AXS D8 Advance Powder X-ray Diffractometer (CuK α source, $\lambda=1.5418$ Å). Energy dispersive X-ray (EDX) measurements were carried out with an X-ray Microanalyzer (Oxford Scientific) attached to a JSM-840 Scanning Electron Microscope (JEOL). The specific surface area was determined by N₂ adsorption [Brunauer, Emmett, and Teller (BET) method] using a Micrometrics Gemini instrument (USA). Differential scanning calorimetric (DSC) analysis was carried out with a Mettler Toledo TC 15 system using a stream of nitrogen (20 ml/min) at a heating rate of 4°C/min up to 600°C. The morphology of the materials was studied by transmission electron microscopy (TEM; JEOL-JEM 100SX microscope, working at a 100-kV accelerating voltage). High-resolution TEM (HRTEM) images were obtained using a JEOL 2100 with 200 kV accelerating voltage. Raman spectra were measured by an OLYMPUS BX41 Raman microscope from Jobin Yvon Horiba, France, using a 514.5-nm laser beam.

All the preparations for the electrochemical measurements were carried out under highly pure argon atmosphere (O₂ and H₂O levels <5 ppm in a VAC, Inc. glove box). The electrochemical measurements were carried out using equipment from Maccor, Inc. (Model 2000, multichannel battery analyzer) and EG&G, Inc. (VMP2 multichannel potentiostat).

Results and discussion

Synthesis and characterization

The irradiation of solutions containing thiorea and SnCl₂ in ethylene glycol (see “Experiments” section) for any period between 10 and 40 min produced pure nanocrystalline powder having an orthorhombic structure whose XRD patterns are fully consistent with JCPDS No. 39-0354. The synthesis of SnS₂ produced an amorphous phase (as realized by XRD). Heating this product (amorphous powder) up to 450°C produced a nanocrystalline, pure hexagonal SnS₂ phase, whose XRD patterns are fully

consistent with JCPDS No. 23-0677. Indeed, the study of the as-synthesized (amorphous) SnS₂ product by DSC clearly showed thermograms characterized by a broad exothermic band from 360° to 440°C, with a sharp peak at 420°C. This behavior is consistent with the phase transition from amorphous to hexagonal structure occurring between 400° and 450°C, as was evident from the aforementioned studies of these materials by XRD. Cooling and a second heating cycle of these samples produced featureless thermograms, which indicate the irreversibility of the transition of the as-synthesized SnS₂ material from the amorphous to the hexagonal phase.

The average size of the SnS and the crystalline SnS₂ particles obtained herein could be calculated from the XRD patterns by the Debye-Scherrer (DS) equation and are given in Table 1. Raman spectra of the crystalline SnS₂ powder exhibit an intense peak at about 314 cm⁻¹, corresponding to an A_{1g} vibration mode, according to the group theory analysis by Lucovsky et al. [27]. The absence of the expected 210 cm⁻¹ peak related to the first-order E_g mode of crystalline SnS₂ is attributed to the nanosize effect, according to Abello et al. [28].

The BET surface area of the as-prepared (crystalline) SnS and the crystalline SnS₂ was usually 5–6 and 92 m² g⁻¹, respectively. The low surface area of the SnS may be due to the aggregated nature of the crystalline product. The high surface area of the SnS₂ is due to the flakelike morphology of the crystalline nanoparticles, and the BET surface areas of the as-synthesized and annealed samples also appear in Table 1 along with their particle size from TEM.

Figure 1a–c presents TEM micrographs of as-synthesized SnS particles collected after 10, 20, and 40 min of microwave irradiation. All these as-synthesized SnS powders are crystalline (confirmed by XRD). The TEM images also demonstrate the flakelike morphology of the SnS particles (thin flaky crystals about 50–500 nm wide). It is also clear that further irradiation beyond 10 min does not change the properties of the SnS products. Figure 1d,e shows representative HRTEM images of flakelike SnS particles and their lattice planes. The lattice plane of (111), with an interplanar spacing of 0.288 nm (compared with the theoretical interplanar spacing of 0.2835 nm) is displayed in Fig. 1e. The corresponding selected area electron diffraction (SAED) pattern is shown in Fig. 1f. This indeed illustrates that the as-synthesized material is crystalline and can be indexed to orthorhombic SnS. These

Table 1 Particle size and BET surface area from microwave-assisted synthesized tin sulfides

Sample no.	Product	Particle size (nm) from XRD	Particle size (nm) from TEM	BET surface area (m ² g ⁻¹)
1	SnS (10) ^a	36–39	50–500 ^b	6
2	SnS (20) ^a	37–40	50–500 ^b	6
3	SnS (40) ^a	38–40	50–500 ^b	5
4	Annealed SnS ₂ ^c	38–42	70–300 ^b	92

^aThe number in parenthesis is the irradiation period (minutes)

^bThese particles are in fact agglomerates of nanocrystals. We refer in this table to the longest dimension of the particles

^cThe annealed product of the as-synthesized amorphous SnS₂ material collected after 40 min of microwave irradiation time. The sample was heated at 425°C for 1 h under argon

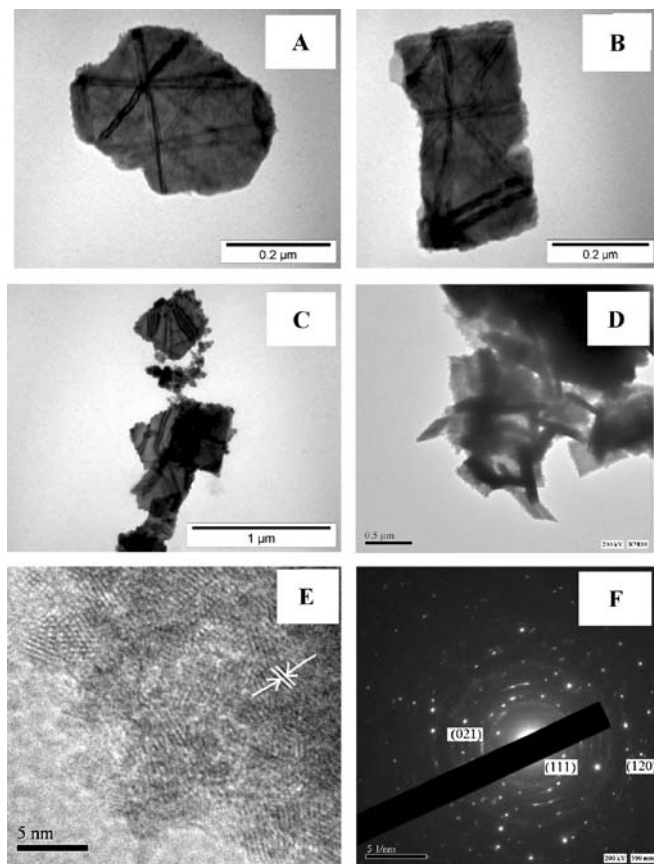


Fig. 1 Low-resolution transmission electron microscopy (LRTEM) images of as-synthesized SnS after **a** 10 min, **b** 20 min, and **c** 40 min of microwave heating. HRTEM image of **d** as-synthesized SnS. **e** HRTEM lattice planes are clearly resolved. **f** Corresponding selected area electron diffraction pattern of SnS after 40 min of microwave heating

microscopic studies show that the SnS particles are in fact agglomerates of nanocrystals. EDX measurements of SnS crystals indicate that they contain 79 wt% Sn and 21 wt% S, compared to the theoretical values 78.8 and 21.2%, respectively. Hence, all the above-reported measurements indicate that we indeed obtain stoichiometric SnS.

Figure 2a–d shows representative TEM images of as-synthesized and annealed SnS₂ materials. The TEM images of the as-synthesized SnS₂ (Fig. 2a,b) also show a flakelike morphology with many irregular shapes on a nanometer scale. These thin, flaky particles are 70–300 nm in length and 5–10 nm thick. After annealing, the flakelike morphology of the SnS₂ (Fig. 2c,d) remains almost unchanged. The HRTEM image (Fig. 2e) of a single nanoflake SnS₂ crystal shows clearly resolved interplanar distances, $d_{001}=0.6$ nm, as compared with the theoretical 0.589 nm for the hexagonal SnS₂ phase. The intense rings, seen in the SAED patterns (Fig. 2f), further verify the hexagonal structure of the annealed SnS₂. The EDX measurement of individual nanoflakes confirmed the SnS₂ stoichiometry: 64.6 wt% of Sn and 35.4 wt% of S, compared to the theoretical values 65 and 35%, respectively. The quantitative analysis by EDX was obtained using a library of

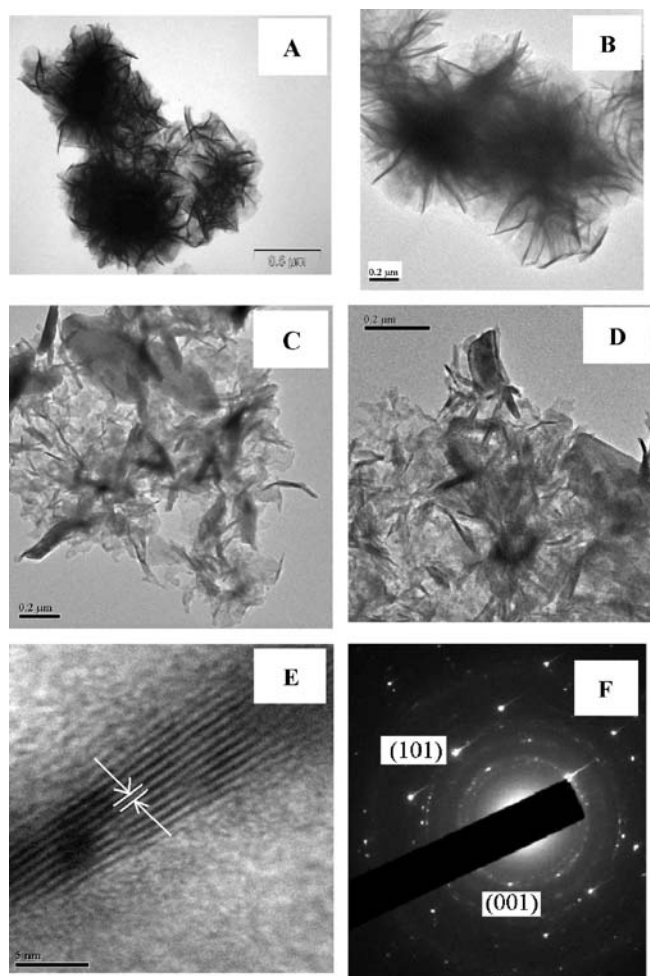


Fig. 2 HRTEM images of **a, b** as-synthesized **c, d** calcined SnS₂ heated at 425°C in Ar for 1 h. **e** HRTEM lattice planes are clearly resolved. **f** Corresponding selected area electron diffraction pattern of SnS₂

standards from JEOL, Inc. It should be noted that the difference in size obtained by the analysis of the XRD patterns and by TEM images is due to the high orientation of the flaky crystals. The particle size obtained by calculations based on the XRD data probably reflects mostly the small dimensions of the particles (thickness), while the dimensions seen in TEM are the large dimensions, namely, the length of the particles.

Mechanism of formation The exact mechanism for the solvothermal synthesis of crystalline SnS and amorphous SnS₂ flakelike structures using microwave irradiation needs further investigation. The following proposed mechanism is based on previous reports related to conventional heating methods [29–32].

We suggest a two-stage process: In the first step (nucleation stage), a tin-thiourea complex is formed. It dissolves in ethylene glycol and undergoes microwave-induced decomposition, leading to a rapid generation of SnS or SnS₂ nuclei. In the second step, the tin sulfide nuclei grow preferentially along the (001) crystal plane, which results in the formation of single-crystalline flakes.

Microwave irradiation plays a critical role in both of the above two stages. In these reactions, temperature is the dominant factor affecting the reactivity. The interaction between the high-frequency electromagnetic radiation (2.45×10^9 Hz) and the permanent dipole moment of the precursors results in molecular rotations, which lead to the rapid volumetric heating of the liquid phase, which is capable of driving the thermal decomposition of the thiourea complex to produce tin sulfide nuclei. Due to the relative stability of the complexes, decomposition proceeds relatively slowly and produces a small number of nuclei in the glycol solution, which may be favorable for the oriented growth of the flakelike structures. Compared to conventional heating methods, microwave dielectric heating presents a much more rapid and simultaneous nucleation due to the fast and homogeneous heating effects of microwaves. We suggest that the high microwave susceptibility of EG (dielectric constant $\epsilon=39$) makes it an excellent microwave-absorbing agent, thus leading to high heating rates (because of high boiling point, 196–198°C) and significantly shortened reaction times. Microwave irradiation is also capable of inducing the preferential 2D growth of the tin sulfide materials. One possible hypothesis for the microwave-induced effect is the generation of localized high temperatures and pressures at the reaction sites that enhance the rate of reaction, which is favorable for the 2D growth. The possible reason for the formation of crystalline SnS and amorphous SnS₂ flakelike structures may be due to the high microwave susceptibility power of SnS compared to SnS₂. The exact mechanism on the morphology of SnS and SnS₂ flakelike structures is still under investigation.

It should be noted that in parallel to the studies reported herein, Chen et al. [22] reported on the synthesis of SnS and SnS₂ using microwave irradiation of similar precursors as was used in this work. That work [22] differs considerably from the present one in terms of product distribution, morphology of products, parameters studied, lack of mechanistic discussion, and studies of possible applications. In any event, the publication of Chen et al. [22] confirms the main theme of this paper, namely, that microwave-based synthesis is a reliable route for the easy

preparation of SnS, which is a highly interesting anode material for rechargeable Li batteries, as discussed below.

Electrochemical measurements

The research reported herein did not include prolonged cycling of SnS or SnS₂ electrodes because such experiments are significant only if the study includes a rigorous optimization of the composite electrodes. The stability of capacity and capacity fading of composite electrodes for Li battery systems upon prolonged cycling depends on several engineering factors: amount of binder and conductive additives, the morphology and size of the latter component, thickness, porosity, the application of pressure during preparation, and more. In the present study, we concentrated on two major factors: the nature of the active mass and the electrolyte solutions. As presented herein, the impact of these factors is clearly demonstrated even during relatively short cycling experiments.

Figures 3 and 4 show typical potential profiles and cycling behavior of SnS electrodes in PC and PC-EC (LiClO₄) solutions. The first cathodic polarization of these electrodes (see insert in Figs. 3, 4) leads to an obvious irreversible conversion of the SnS to Sn + Li₂S and to surface reactions due to the reduction in solution species, which form passivating surface films of the reduction in SnS₂ [33]. The irreversible capacity may reach values of 1,000–1,400 mAh/g. After the initial formation of Li₂S and passivating surface films, these electrodes insert lithium reversibly at capacities and stability that depend very strongly on the composition of the electrolyte solution. The highest capacity (<600 mAh/g) was obtained in the EC-PC/LiClO₄ solution (Fig. 4). Cycling SnS electrodes in EC-DMC solutions (not presented herein) led to poor capacity (≈ 200 mAh/g).

Figure 5 compares potential profiles of SnS, and crystalline and amorphous SnS₂ electrodes in an EC-PC/LiClO₄ solution during the first two galvanostatic cycles. There are pronounced differences between the potential profiles of SnS and SnS₂ electrodes during the first cathodic polarization. Both show sloping plateaus at potentials below 1.5 V (Li/Li⁺). These plateaus, of course, reflect the

Fig. 3 Capacity vs cycle number for an SnS composite electrode in 1 M LiClO₄/PC solution at different charge/discharge rates. The *insert* shows a typical potential profile

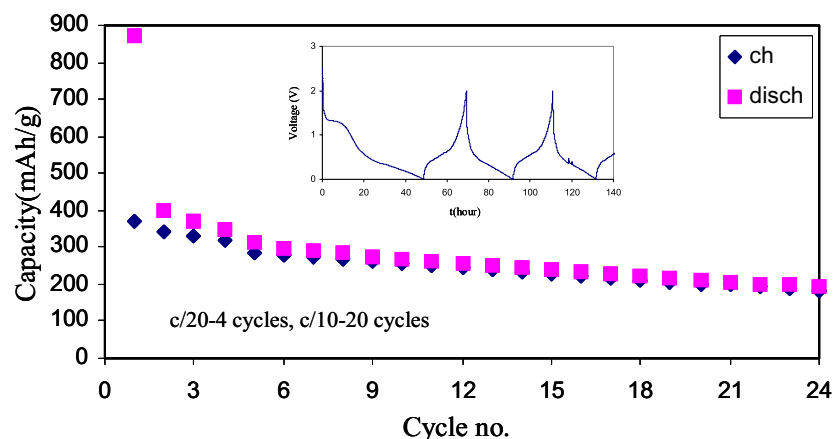
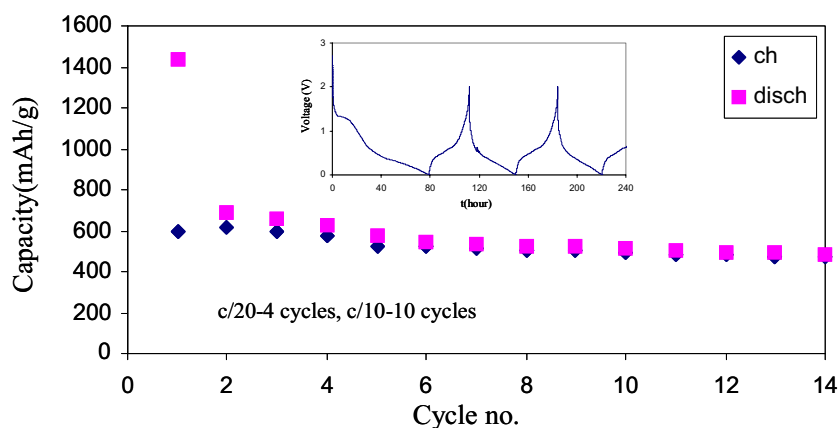


Fig. 4 Capacity vs cycle number for an SnS composite electrode in 1 M LiClO₄/EC:PC 1:1 solution at different charge/discharge rates. The *insert* shows a typical potential profile



formation of Li₂S and Sn by lithiation of SnS and SnS₂. The latter process should consume twice the amount of charge of the former one. However, these lithiated processes are complicated by the parallel reduction in solution species, which are reflected also by the sloping potential profile of the first cathodic polarization in PC, PC-EC, or EC-DMC LiClO₄ solutions. Only with a LiBOB/EC-DMC solution could a stable reversible capacity around 100 mAh/g be obtained with crystalline SnS₂ electrodes. It should be noted that the irreversible capacity in this case was relatively low (≈ 750 mAh/g), which correlates well with the behavior of graphite electrodes in LiBOB solutions [34].

Amorphous SnS₂ electrodes showed a much better reversible behavior, compared to the crystalline phase, but worse than that of SnS electrodes. However, as expected, the irreversible capacity of the SnS₂ electrodes is higher than that of SnS electrodes. The cycling behavior and stability of the SnS₂ electrodes also depend on the solution composition (as is the case for SnS).

Figure 6 demonstrates the best performance obtained with amorphous SnS₂ electrodes (EC-DMC 1M LiClO₄). We therefore have to conclude that SnS₂ should not be regarded as a promising anode material for Li batteries. However, SnS can be considered as an interesting material that deserves further study.

The inferiority of SnS₂ as a lithium insertion material (in terms of capacity and reversibility) compared to SnS

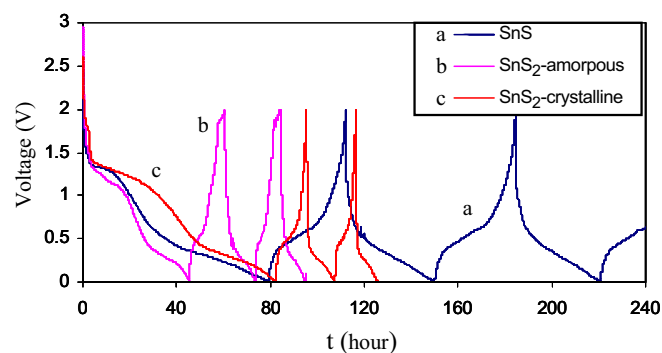
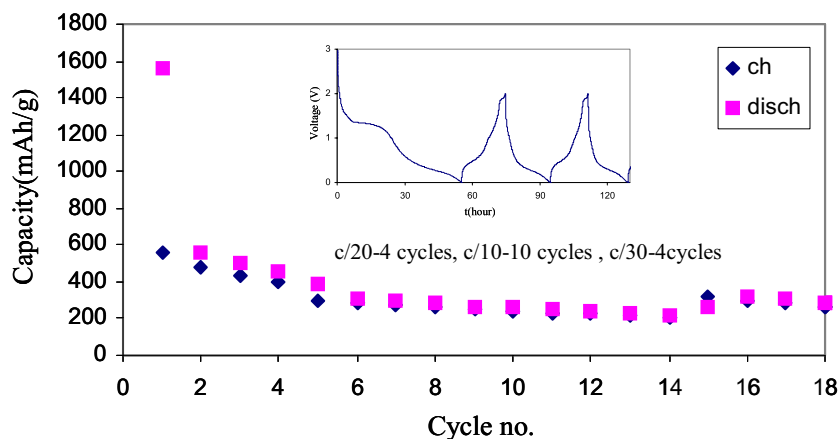


Fig. 5 Comparison between SnS composite electrode in 1 M LiClO₄/EC:PC 1:1 solution, amorphous SnS₂ and crystalline SnS₂ composite electrodes in the same electrolyte solution by typical potential profiles

should be attributed to the impact of the ratio between the active element Sn and the “spectator” element S in the SnS_x compounds. The latter element is important for the formation of Li₂S matrix which is probably critical for the overall integrity of the active mass (i.e., it is highly advantageous having an active mass comprising nanoparticles of Li_xSn embedded in a matrix of Li₂S). However, another critical need is a good interparticle electrical contact. In this respect, too high ratio between Li₂S and Li_xSn may be detrimental for the performance. We can speculate that the superiority of amorphous SnS₂ compared to the crystalline materials relates to the better electrical interparticle contact when the pristine material is amorphous (yet, the high S/Sn ratio makes it inferior to SnS). Similar trend and explanations were relevant to our previous studies of SnO and SnO₂ as anode materials for rechargeable Li batteries [35, 36].

It is clear the impact of the composition of the electrolyte solution on the performance of SnS electrodes is highly important. It is also clear that the working active mass of the electrodes are Li-Sn nanoparticles embedded in a matrix comprising Li₂S and a variety of solution-reduction products. Figure 7 shows typical Fourier transform infrared (FTIR) spectra of particles scraped from cycled SnS electrodes in EC-DMC/LiPF₆ and in EC:PC (1:1)/LiClO₄ solutions (as indicated), pelletized with KBr (transmission mode). These spectra include typical peaks of ROLi, ROCO₂Li, and Li₂CO₃ species (indicated in Fig. 7), which are the typical reduction products of alkyl carbonate solvents in the presence of Li ions [37]. The same species compose the surface films formed on lithium metal, lithiated carbons [38], and nonactive metals polarized to low potentials in aprotic Li salt solutions based on alkyl carbonate solvents [39]. It should be noted that FTIR spectra measured from particles scraped from cycled SnS or SnS₂ electrodes in all the other above-mentioned solutions were generally similar to the spectra of Fig. 7. Hence, the surface chemistry of the composite SnS or SnS₂ electrodes in the standard alkyl carbonate solutions tested herein is generally as expected from previous studies of composite carbonaceous (or nonactive metal) electrodes, polarized cathodically in these solutions [34–37]. In addition, by the FTIR analysis of SnS and SnS₂ particles that were in contact with the solvents, we verified that SnS

Fig. 6 Capacity vs cycle number for an amorphous SnS₂ composite electrode in 1 M LiClO₄/EC:DMC 1:1 solution at different charge/discharge rates. The *insert* shows a typical potential profile



or SnS₂ does not react directly with alkyl carbonate solvents (note that SnS or SnS₂ might have nucleophilic activity with the highly electrophilic alkyl carbonates).

The pronounced dependence of the performance of these electrodes on the composition of the electrolyte solutions is probably related to the specific surface chemistry that is developed in solutions. The FTIR spectroscopic data obtained herein is not specific enough to clearly differentiate among the exact surface species formed in each solution, as the IR spectra of many ROLi or ROCO₂Li species have many similar features [37–40]. However, we can explain the superior behavior of SnS electrodes in the EC-PC LiClO₄ solution based on previous studies and understanding. Major reduction products of PC and EC in the presence of Li ions are Li-dialkyl carbonate species [41] [e.g., (CH₂OCO₂Li)₂, in the case of EC reduction]. It is generally accepted now that the typical IR spectra of ROCO₂Li species relate to intermolecular structures in which Li ions bridge between -OCO₂⁻ groups [42, 43]. Hence, when dicarbonate surface species are formed, they may form lateral networks that can passivate active electrodes (lithium, lithiated carbons, and other lithiated species at low potentials) [44].

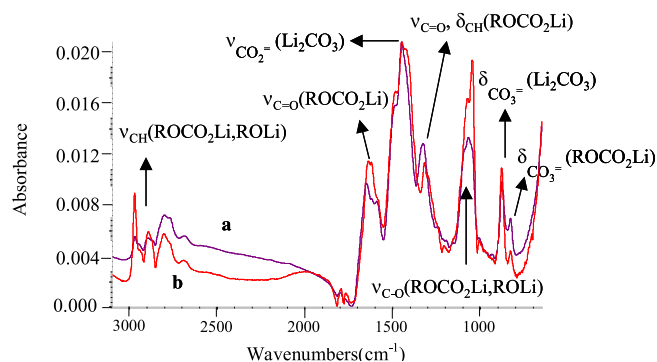


Fig. 7 FTIR spectra measured by transition mode, obtained from cycled composite SnS electrode in different solutions. **a** In EC:DMC/LiPF₆. **b** In EC:PC (1:1)/LiClO₄. Particles of active mass were scraped from dry electrodes after cycling and were measured palletized with KBr (transmission mode). Some peak assignments are presented

Lateral networks of Li alkyl dicarbonate species are expected to have some degree of flexibility and thus may be able to accommodate pronounced volume changes during lithiation-delithiation reactions (e.g., upon intercalation, alloying formation). The limitations in capacity, stability, and cycleability of Li-Sn electrodes are attributed to the pronounced volume changes that occur upon lithiation of tin and its reverse process [45]. These volume changes are detrimental to the passivation of Li-Sn electrodes by surface films and hence lead to continuous reactions between lithiated tin (a highly reductive compound) and solution species. Continuous reactions with solution species mean loss of active lithium and the formation of active mass particles electrically isolated from the current collector due to their coverage by insoluble products of the reactions between Li-Sn and solution species, mostly solvent molecules. Hence, the quality of the passivating surface films initially formed on Li-Sn electrodes is critical for their performance. In this respect, surface species containing two Li-carbonate groups (reduction products of both EC and PC [41]) are very advantageous, as explained above.

These results encourage further study of these systems, especially the optimization of the composition of the electrolyte solutions, in order to promote the best surface chemistry suitable for the good passivation of Li-Sn particles. Possible directions may be the use of reactive additives that react predominantly on the electrodes' surface, thus forming surface films with superb properties, in a similar manner to the use of vinylene carbonate as an additive that stabilizes lithiated graphite electrodes [46].

Finally, a major problem in the use of an active mass such as SnS is the high initial irreversible capacity due to the necessary formation of Li₂S and the consumption of active lithium and solution species for the formation of passivating surface films. In Li-ion batteries, where the source of lithium is the LiMO_x cathode, the huge irreversible capacity of all tin-based electrodes is totally unacceptable. A possible solution to this problem may be a prelithiation of these electrodes by a short with lithium metal. It is possible to attach a measured amount of metallic lithium to the composite SnS electrode. The structure of these electrodes allows all the active mass to be in electrical

contact with any piece of lithium attached to the electrode. As the solution is introduced, both the active mass (SnS) and the lithium metal become electrochemically connected by the electrolyte solution, and thus, a simple galvanic cell is formed in which the Li metal dissolves (anodic process) in parallel to all the desirable cathodic processes that take place (lithiation of tin, Li_2S formation, and reduction in solution species to form passivation surface films). Since such processes are fast, take place as soon as the solution is introduced, and consume all the metallic lithium, the initial presence of metallic lithium upon assembling the cells should not be considered a safety problem. It should be noted that all kinds of Li batteries contain an excess of solution; therefore, the obvious consumption of solution species in these prelithiation processes should not at all be a problem.

We carried out several experiments in light of the above and found this approach to be viable and logical.

Conclusion

We developed easy, fast, and cheap syntheses of nanometric flakes of SnS and SnS_2 materials in a simple microwave oven using SnCl_2 or SnCl_4 and thiourea as precursors in ethylene glycol as a medium and a mild reducing agent. The SnS is formed as a crystalline orthorhombic phase in a morphology of agglomerated flakes. The SnS_2 is formed as an amorphous phase, which, upon heating up to 425°C , changes to a crystalline hexagonal phase. Composite electrodes comprising SnS and SnS_2 as the active mass (also containing a few percent of carbon and a PVDF binder) were tested as Li insertion electrodes in several commonly studied Li salt solutions for potential use as negative electrodes in secondary Li batteries. The parameters of interest were capacity and stability upon repeated lithiation (charge)-delithiation (discharge) cycling. A very poor performance was obtained with electrodes comprising SnS_2 . The amorphous SnS_2 electrodes behave better than the latter ones, but their behavior is pronouncedly inferior compared to that of the SnS electrodes.

The performance of all these electrodes was found to be strongly dependent on the composition of the electrolyte solutions. The best performance of the SnS electrodes was obtained in EC-PC/ LiClO_4 . We attribute this to the surface chemistry of active electrodes in this solution, namely, the formation of highly passivating surface films composed of Li propylene and ethylene dicarbonates, which are major reduction products of PC and EC, respectively, in LiClO_4 solutions. Such surface species containing two Li-carbonate groups are expected to precipitate as networks in which Li ions bridge between carbonate groups. These films should provide good passivation and allow a very good Li-ion transport through them.

FTIR studies of cycled electrodes indeed confirmed the formation of ROCO_2Li as major surface species in all the electrolyte solutions studies (all comprise alkyl carbonate solvents). These results encourage further optimization of

these systems in terms of the structure of the composite electrodes and the composition of the electrolyte solutions.

We suggest herein the prelithiation of these electrodes (in the authentic solution, in the battery) with metallic lithium as a practical solution for the problem of the high initial irreversible capacity.

Acknowledgement Partial support for this work was obtained from the EC within the framework of the 5th Program of the Nanobatt Project.

References

1. Heath JR (1999) *Acc Chem Res* 32:387
2. Gorer S, Hodes G (1994) *J Phys Chem* 98:5338
3. Empedocles SA (1999) *J Phys Chem B* 103:1826
4. Ludolph B, Malik MA, O'Brien P, Revaprasadu N (1998) *Chem Commun* 17:1849
5. Alivisatos AP (1996) *Science* 271:933
6. Jun YW, Jung YY, Cheon JJ (2002) *J Am Chem Soc* 124:615
7. Shiang JJ, Kadavanich AV, Grubbs RK, Alivi-Satos AP (1995) *J Phys Chem* 99:17417
8. Ahmadi S, Wang ZL, Green TC, Henglein A, El-Sayed, MA (1996) *Science* 272:1924
9. Bube RH (1960) *Photoconductivity of solids*. Wiley, New York, p 233
10. Nair MTS, Nair PK (1991) *Semicond Sci Technol* 6:123
11. Prince MB (1955) *J Appl Phys* 26:534
12. Loferski JJ (1956) *J Appl Phys* 27:777
13. Agarwal A, Patel PD, Lakshminarayana D (1994) *J Cryst Growth* 142:344
14. Lokhande CD (1990) *J Phys D Appl Phys* 23:703
15. Domingo G, Itoga RS, Cannewurf CR (1966) *Phys Rev* 143:536
16. Chu DR, Walser M, Bene RW, Courtney TH (1974) *Appl Phys Lett* 24:479
17. Polarz S, Smarsly B, Goltner C, Antonietti M (2000) *Adv Mater* 12:1:503
18. Morales J, Perez VC, Santos J, Tirado LJ (1996) *J Electrochem Soc* 143:2847
19. Szabó DV, Vollath D (1999) *Nanostruct Mater* 12:597
20. Baghurst DR, Mingos DMP (1991) *Chem Soc Rev* 20:1
21. Mingos DMP (1994) *Chem Ind* 15:596
22. Chen D, Shen G, Tang K, Lei S, Zheng H, Qian Y (2004) *J Cryst Growth* 260:469
23. Momma T, Shiraishi A, Yoshizawa A, Osaka T, Gedanken A, Zhu J, Sominski L (2001) *J Power Sources* 97:198
24. Mukaibo H, Yoshizawa A, Momma T, Osaka T (2003) *J Power Sources* 119:60
25. Jayalakshmi M, Rao MM, Choudary BM (2004) *Electrochem Commun* 6:1119
26. Palchik O, Felner I, Kataby G, Gedanken A (2000) *J Mater Res* 15:2176
27. Lucovsky G, Mikkelsen JC, Liang WY Jr, White RM, Martin RM (1976) *Phys Rev B* 14:1663
28. Abello L, Bochu B, Gaskov A, Koudryavtseva S, Lucazeau G, Roumyantseva M (1998) *J Solid State Chem* 135:78
29. He R, Qian X, Yin J, Zhu Z (2003) *J Cryst Growth* 252:505
30. Wang H, Zhu J-M, Zhu J-J, Yuan L-M, Chen HY (2003) *Langmuir* 19:10993
31. Kerner R, Palchik O, Gedanken A (2001) *Chem Mater* 13:1413
32. Galema SA (1997) *Chem Soc Rev* 26:233 (and the references therein)
33. Brousse T, Lee SM, Pasquereau L, Defive D, Schleich DM (1998) *Solid State Ionics* 115:51
34. Xu K, Zhang S, Poese BA, Jow TR (2002) *Electrochem Solid State Lett* 5:A259

35. Zhu J, Lu Z, Aruna ST, Aurbach D, Gedanken A (2000) *Chem Mater* 12:2557
36. Aurbach D, Nimberger A, Markovsky B, Levi E, Sominski E, Gedanken A (2002) *Chem Mater* 14:4155
37. Aurbach D, Markovsky B, Schechter A, Ein-Eli Y, Cohen H (1996) *J Electrochem Soc* 143:3809
38. Aurbach D, Gofer YJ (1991) *J Electrochem Soc* 138:3529
39. Aurbach D, Ein-Eli Y, Chusid O, Babai M, Carmeli Y, Yamin H (1994) *J Electrochem Soc* 141:603
40. Aurbach D, Daroux ML, Faguy P, Yeager E (1991) *J Electroanal Chem* 297:225
41. Aurbach D, Gofer Y, Ben-Zion M, Aped P (1992) *J Electroanal Chem* 339:451
42. Matsuta S, Asada T, Kitaura K (2000) *J Electrochem Soc* 147:1695
43. Wang YX, Balbuena P (2002) *J Phys Chem B* 106:4486
44. Aurbach D, Markovsky B, Gamolsky K, Levi E, Ein-Eli Y (1999) *Electrochim Acta* 45:67
45. Huggins RA (1999) In: Besenhard JO (ed) *Handbook of battery materials*, part 3, chap 4. Wiley, Weinheim and New York, p 370
46. Aurbach D, Gamolsky K, Markovsky B, Gofer Y (2002) *Electrochim Acta* 47:142